J|A|C|S
ARTICLES
Published on Web 07/14/2006

Structural Characterization of Ultrasmall Superparamagnetic Iron Oxide (USPIO) Particles in Aqueous Suspension by Energy Dispersive X-ray Diffraction (EDXD)

Mariagrazia Di Marco,[†,‡] Marc Port,[‡] Patrick Couvreur,[†] Catherine Dubernet,[†] Paolo Ballirano,[§] and Claudia Sadun*[,||]

Contribution from the Faculté de Pharmacie, Université de Paris Sud, UMR CNRS 8612, tour D5, 5 Rue JB Clément, 92926 Châtenay Malabry, France, Guerbet, Centre de Recherche BP 50400, 95943 Roissy CdG Cedex, France, Dipartimento di Scienze della Terra Università di Roma "La Sapienza" P.le A. Moro, 5 I-00185 Roma, Italy, and Dipartimento di Chimica, CNISM Consorzio Nazionale Interuniversitario per le Scienze Fisiche della Materia, Università degli Studi di Roma "La Sapienza" P.le A. Moro, 5 I-00185 Roma, Italy

Received March 10, 2006; E-mail: c.sadun@caspur.it

Abstract: Ultrasmall superparamagnetic iron oxide (USPIO) particles were structurally characterized in situ in an aqueous dilute suspension by energy dispersive X-ray diffraction (EDXD) and ex situ as powders obtained by lyophilization of the suspension by angular dispersive X-ray diffraction (ADXD) at 20 °C. Structural parameters obtained by the Rietveld method on ADXD data were used as starting parameters for modeling the structure of the particles in suspension. Although each particle is a single crystal, as evidenced by conventional X-ray diffraction, our results indicate that the structural order, specific to a crystal, does not extend to the entire volume of the particle. In fact, each individual particle, averagely, has a crystalline structural extension ca. 4.0 nm smaller than the apparent dimensions obtained by both ADXD and TEM (ca. 8.0 nm).

Introduction

Among the materials showing magnetic properties, γ-Fe_2O_3 nanoparticles have recently been subjected to a large number of investigations.[1−3] In fact, ferrofluids can be obtained by dispersing magnetic nanoparticles in water, after surface modification to prevent aggregation. They may be used in biological applications, such as drug targeting and diagnostics. Ultrasmall superparamagnetic iron oxide (USPIO) particles are now efficient contrast agents used to enhance relaxation differences between healthy and pathological tissues, due to their high saturation magnetization, high magnetic susceptibility, and low toxicity. The biodistribution and resulting contrast of these particles are highly dependent on their synthetic route, shape, and size (the maximum dimension of the particle). Consequently, an in-depth knowledge of their physicochemical and structural properties is the key to understanding the biological and magnetic properties of USPIO.[4−6]

Magnetization measurements have shown that the saturation magnetization of γ-Fe_2O_3 nanocrystals, small enough to show superparamagnetic properties, decreases with decreasing particle size. Although the magnetic properties of fine particles are strongly influenced by finite size and surface effects, very different magnetic properties have been observed in materials with similar nominal grain size but produced by different synthetic routes. The reduction of the saturation magnetization observed in the smallest nanoparticles is difficult to interpret by considering only the finite size and surface effects.[7,8] To explain this phenomenon, several hypotheses concerning the cationic disorder in the entire volume of the crystal structure have been proposed. However, there is no unequivocal way of clearly differentiating the individual contributions arising from finite size, surface effects, and structural disorder of the particles to identify their effect on specific magnetic properties.[9,10]

The present study was aimed at improving the understanding of fine structural details of single small particles measuring less than 10 nm, which exhibit material properties very different from those of the bulk materials. These nanoparticles may be considered to be a less-ordered system, which is neither

[†] Université de Paris Sud.
[‡] Guerbet, Centre de Recherche.
[§] Scienze della Terra, Università di Roma.
[||] Chimica, Università di Roma "La Sapienza".

(1) Skomski, R. *J. Phys.: Condens. Matter.* **2003**, *15*, R841.
(2) Batlle, X.; Labarta, A. *J. Phys. D: Appl. Phys.* **2002**, *35*, R15.
(3) Kodama, R. H.; Berkowitz, A. E. *Phys. Rev. B* **1999**, *59*, 6321.
(4) Guptaa, A. K.; Gupta, M. *Biomaterials* **2005**, *26*, 3995.
(5) Tartaj, P.; Morales, M. P.; Veintemillas-Verdaguer, S.; Gonzalez-Carreño, T.; Serna, C. J. *J. Phys. D: Appl. Phys.* **2003**, *36*, R182.
(6) Tartaj, P.; Morales, M. P.; Veintemillas-Verdaguer, S.; Gonzalez-Carreño, T.; Serna, C. J. *J. Magn. Magn. Mater.* **2005**, *290*−*291*, 28.
(7) Morales, M. P.; Veintemillas-Verdaguer, S.; Montero, M. I.; Serna, C. J.; Roig, A.; Casas, Ll.; Martinez, B.; Sandiumenge, F. *Chem. Mater.* **1999**, *11*, 3058.
(8) Chatterjee, J.; Haik, Y.; Chen, C. J. *J. Magn. Magn. Mater.* **2003**, *257*, 113.
(9) Morales, M. P.; Sernaz, C. J.; Bødkerx, F.; Mørup, S. *J. Phys.: Condens. Matter.* **1997**, *9*, 5461.
(10) Iglesias, O.; Labarta, A. *Phys. Rev. B* **2001**, *63*, 184416-1.

10.1021/ja061674y CCC: $33.50

completely crystalline nor completely amorphous. For this reason, two kinds of analyses were chosen to characterize their structure, one especially suited to crystalline systems and the other to amorphous ones. The structure of the particles was investigated both ex situ as a lyophilized (freeze-dried) powder by angular dispersive X-ray diffraction (ADXD) and in situ as the aqueous suspension intended for clinical purposes, using a noncommercial energy dispersive instrument (EDXD). Structural data obtained for the nanoparticles by ADXD were subsequently employed to build a structural model for the aqueous suspension. Moreover, this technique, as well as TEM, has been used to estimate the apparent size of the nanoparticles. Analysis of the nanoparticles directly in suspension cannot be carried out by conventional X-ray diffraction techniques. However, this can be done by EDXD, a technique that has been widely employed in the structural characterization of amorphous samples, liquids, and biological systems,[11−13] and potentially enables the analysis of all the systems with a low degree of crystallinity. Its particular geometric properties allow the placement of liquid samples in a closed cell and much shorter acquisition times than those typical of any other in-house apparatus.

Experimental Section

Nanoparticle Characterization. The γ-Fe_2O_3 nanoparticles were synthesized via aqueous precipitation of magnetite, according to a previously reported method,[14] and followed by an oxidation to maghemite under acidic conditions. The ferrimagnetic fine particles were then coated with an organic layer (phosphonate) in order to prevent coagulation of the colloids.

Both the Fe core and the coating content of the γ-Fe_2O_3 nanoparticles in aqueous suspension were determined by inductively coupled plasma atomic emission spectrophotometry (ICP-AES) using a Varian Liberty 150. Average crystal size was evaluated by transmission electron microscopy (TEM). For this purpose, samples were prepared from the particle suspension by drying on carbon-coated holey copper grids.

The structure of the particles was characterized using both angular dispersive X-ray diffraction (ADXD) and EDXD. ADXD was carried out ex situ on powders obtained by lyophilization of the water suspension, whereas EDXD was carried out in situ directly on the aqueous suspension.

ADXD. ADXD data were collected on a Bruker-AXS D8Focus automated powder diffractometer, equipped with Göbel mirrors on the incident beam, Si(Li) Peltier-cooled solid-state detector, and operating in Debye−Scherrer transmission geometry. Data were evaluated by the Rietveld method using both the GSAS crystallographic suite of programs[15] and Topas.[16] The choice of two different software packages was made according to their different approaches to peak shape modeling, a conventional approach in the case of GSAS, and the fundamental parameter approach (FPA)[17] in the case of Topas. In the first case, the peak shape was modeled by means of a function whose parameters were, in some way, related to microstructural features of the sample (size and strain) and to instrumental properties. FPA is, on the contrary, a convolution approach in which the peak shape is synthesized from a priori known features of the diffractometer (i.e., the emission profile of the source, the width of the slits, the angle of divergence of the incident beam), and the microstructural features of the specimen. This approach is believed to improve the stability and the quality of the refinement, especially with respect to the extraction of microstructural parameters.

The powder was loaded inside a 0.2 mm diameter borosilicate glass capillary that was mounted and aligned on a standard goniometer head. The effective absorption of the cylindrical sample[18] was refined during the least-squares process. In the case of the refinement carried out by the GSAS software, the peak shape was modeled with the TCH pseudo-Voigt function.[19] The refined variables were the angle-independent Gaussian parameter GW and the LX (1/cos θ-dependent) Lorentzian parameter. The latter contains information about the coherency domain size that may be extracted via the Scherrer equation. We were not able to refine any strain-dependent parameter, possibly because of correlation. The background was fitted with a 30-term Chebyshev polynomial of the first kind. Such a large number of terms were required to properly model the amorphous contribution of the capillary. Peak position was corrected for sample displacement from the focusing circle. Cell parameters, fractional coordinates, and displacement parameters were subsequently refined. The presence of preferred orientation was checked by means of the spherical harmonics approach.[20] No improvement of the fit was obtained as a result of a *J* texture index very close to 1. In the case of Topas, as mentioned above, the peak shape was modeled through FPA imposing a simple axial model (12 mm) and the size of divergence/anti-divergence (0.6 mm) and receiving (0.1 mm) slits. Peak broadening was assumed to follow a Lorentzian (size) and a Gaussian (strain) behavior.[21] Refined structural parameters were the same as those in the case of the GSAS software.

EDXD. The suspension (Fe = 0.30 mol/L) placed in a sample holder, suitable for liquid, was analyzed in situ by EDXD at the temperature of 20 °C. Moreover, at the same experimental condition, data for the sample holder and pure water were collected to take into account their contribution. The sample holder consists of organic polymeric material, a Teflon cell with Mylar circular windows, 3 mm path length, 0.8 mL volume.

Diffraction data were acquired by a custom-built energy dispersive X-ray diffractometer.[22] This instrument consists of a Seifert X-ray HV generator supplying a water-cooled tungsten X-ray source, with a maximum power of 3.0 kW. The *bremsstrahlung* component of the X-ray source was used. Operating conditions were as follows: 50 kV high voltage supply, 35 mA current intensity, 15.0−45.0 keV energy range. The counting system consists of a Ge solid-state detector (SSD) connected via an electronic chain to a multichannel analyzer. The diffractometer was fitted with a series of collimating slits placed in front of and behind the sample. Two step-motors move the arms supporting the source and the detector, and an adjustable sample holder was placed in the optical center of the diffractometer.

The total experimental scattering parameter range, $q = 0.16-17.42$ Å^{-1}, was obtained recording spectra at the following measurement angles of 24, 15.5, 8.0, 5.0, 3.0, 2.0, 1.5, 1.0, and 0.5°.

The scattering parameter q could be written as

$$q = \frac{4\pi \sin\theta}{\lambda} = EC \sin\theta$$

where q is expressed in Å^{-1}, λ in Å, E in keV, angles θ in degrees, and the value of the constant C is 1.014.

(11) Sadun, C.; Bucci, R.; Magrì, A. L. *J. Am. Chem. Soc.* **2002**, *124*, 3036.
(12) Caminiti, R.; Carbone, M.; Panero, S.; Sadun, C. *J. Phys. Chem. B* **1999**, *103*, 10355.
(13) Caracciolo, G.; Sadun, C.; Caminiti, R. *Appl. Phys. Lett.* **2004**, *85*, 1630.
(14) Port, M.; Corot, C.; Raynal, I.; Rousseaux, O. U.S. Patent 200425318, Dec. 16, 2004.
(15) Larson, A. C.; Von Dreele, R. B. *1985 GSAS General Structure Analysis System*; LAUR 86-748, Los Alamos National Laboratory, The Regents of the University of California.
(16) *Bruker AXS, 2005; Topas V3: General profile and structure analysis for powder diffraction data*, user's manual; Bruker AXS: Karlsruhe, Germany.
(17) Cheary, R. W.; Coelho, A. A. *J. Appl. Crystallogr.* **1992**, *25*, 109.
(18) Sabine, T. M.; Hunter, B. A.; Sabine, W. R.; Ball, C. J. *J. Appl. Crystallogr.* **1998**, *31*, 47.
(19) Thompson, P.; Cox, D. E.; Hastings, J. B. *J. Appl. Crystallogr.* **1987**, *20*, 79.
(20) Von Dreele, R. B. *J. Appl. Crystallogr.* **1997**, *30*, 517.
(21) Delhez, R.; de Keijser, T. H.; Langford, J. I.; Louër, D.; Mittemeijer, E. J.; Sonneveld, E. J. In *The Rietveld Method*; Young, R. A., Ed.; Oxford University Press: New York, 1993; pp 132−166.
(22) Caminiti, R.; Sadun, C.; Rossi, V.; Cilloco, F.; Felici, R. Patent No. RM/93 01261484, June 23, 1993.

Table 1. Root Mean Square (rms) σ_{ij} Values Used in the Model of γ-Fe_2O_3

range (r, Å)	σ_{ij}
$0 < r \leq 2.20$	0.060
$r > 2.20$	0.120

The experimental data were subsequently corrected normalizing to the incident radiation intensity and dividing by X-ray absorption and polarization coefficients. In addition, the escape peaks were suppressed, and the contributions due to inelastic scattering were subtracted from the observed intensities $I(E, \theta)$.

Atomic scattering factors, $f_h(q)$, were taken from the International Tables for Crystallography Vol. C (Tables 4.2.6.8 and 6.1.1.4).

The static structure function $i(q)$, [u.e. Å^{-1}]

$$i(q) = I_{\text{coh}}(E,\Theta) - \sum f^2_{\text{h}}(q)$$

was then calculated. The radial distribution $D(r)$[el^2 Å 10^2] is

$$D(r) = 4\pi r^2\rho_0 + 2r\pi^{-1}\int_0^{q_{\max}} qi(q)M(q)\sin(rq)dq$$

where ρ_0 is the average electron density of the sample ($\rho_0 = (\sum_{\text{h}} n_{\text{h}} f_{\text{h}}(0))^2 \cdot V^{-1}$, n_{h} the number of atoms of the h atomic species in V the stoichiometric unit volume chosen) and $M(q)$ a modification factor defined by

$$M(q) = [f^2_{\text{Fe}}(0)/f^2_{\text{Fe}}(q)]\exp(-0.01q^2)$$

The experimental radial distribution functions are also shown as $\text{Diff}(r) = D(r) - 4\pi r^2\rho_0$.

Theoretical peaks were calculated performing Fourier transform of a model structure function obtained by the Debye equation for the pair of interactions

$$i(q) = \sum_{ij=1}^{n} f_i f_j \sin(r_{ij}q)(r_{ij}q)^{-1}\exp(-1/2\sigma^2_{ij}q^2)$$

where n is number of atoms in the model, using the same sharpening factor, the same $q_{\max}$ value as that for the experimental data and assuming σ_{ij} is the root-mean-square (rms) variation in the interatomic distance. Instead of using a σ_{ij} value for each distance r_{ij}, we reduced the number of parameters by assigning the same σ value to distances falling within predefined shells. The values selected were typical of rigid structures in comparison to that employed in modeling low ordered materials or liquids.[11,12] The σ values and the predefined ranges used are reported in Table 1.

Only by accessing higher values of q ($q > 10$ Å^{-1}), not available with the usual ADXD monochromatic Cu Kα radiation, radial distribution functions with improved real-space resolution can be obtained. The EDXD, higher-energy X-rays, extends the region of reciprocal space, allowing the success of this kind of analysis. The radial distribution function is carried out in real space and yields the local structure rather than the average crystal structure. Only when the average and local structure are the same (i.e., well-ordered crystals) are the structural parameters obtained from ADXD Rietveld refinement and radial distribution function analysis, on the EDXD data, the same.[23]

Discussion

The structural characterization of the dried sample was carried out by the Rietveld method on conventional ADXD data. Maghemite has an inverse spinel structure, such as magnetite, but differs from the latter by the presence of vacancies within the octahedral site. Its formula can be written as $Fe^{3+}[Fe^{3+}_{5/3}[\ ]_{1/3}]O_4 \equiv Fe^{3+}_8[Fe^{3+}_{4/3}[\ ]_{8/3}]Fe^{3+}_{12}O_{32}$. The vacancies' ordering scheme is closely related to the sample preparation method and results in symmetry lowering and possibly superstructures. The vacancies can be completely random (space group $Fd\bar{3}m$ as in magnetite) or partially ($P4_332$) and totally ordered ($P4_32_12$).[24,25] It has been shown, essentially from combined IR spectroscopy and ADXD, that vacancy ordering occurs only for particles exceeding 5 nm.[7] However, conventional ADXD alone cannot unequivocally define the vacancies' ordering scheme of very small maghemite nanoparticles because of the very large peak broadening (full width at half maximum (fwhm) exceeding 3° 2θ), due to both crystallite size and strain effects, which prevent the detection of the very weak extra-reflection arising from the symmetry reduction. In the present study, different ordering schemes were tested without obtaining any difference in the agreement indices. In the absence of clear indications of the presence of vacancy ordering, we refined the structure in $Fd\bar{3}m$ space group. Rietveld refinements carried out with both the conventional approach and the FPA led to results differing in less than 1σ. The powder consists of particles of nanocrystalline maghemite characterized by isotropic shape (no *hkl* dependence of the peak broadening). The refined cell parameter a was equal to 0.8354(1) nm. This value was only slightly greater ($\Delta a = (a_{\text{n}} - a_{\text{c}})/a_{\text{c}} = 0.001$ with $a_{\text{n}} = a$ parameter of the nanocrystalline sample and $a_{\text{c}} = a$ parameter of the reference crystalline sample) than that reported for microcrystalline samples.[22,24] Moreover, this Δa deviation was smaller than that commonly reported for nanocrystalline samples processed by different techniques.[26] Refined mean Fe^{IV}−O bond distance was 0.188(2) nm, and mean Fe^{VI}−O bond distance was 0.205(1) nm, both in agreement with reference data. A L_{vol} volume-weighted column height of 5.7(5) nm and an ϵ_0 microstrain of 0.10(4) were obtained from FPA refinement. Hypothesizing a spherical morphology of the particles and applying the well-known relation $L_0 = 4/3L_{\text{vol}}$, the L_0 diameter of the particles may be estimated at 7.6(7) nm, in good agreement with TEM data (7.4 nm) (Figure 1). Conversely, in the case of the conventional Rietveld refinement, we obtained a L_{vol} of 8.4(5) nm. The reported difference may be ascribed to the impossibility of modeling the strain broadening; the entire peak broadening was therefore assumed to be size-dependent only. Experimental, calculated, and difference plots for the FPA refinement are reported in Figure 2.

As previously indicated, EDXD was performed in the same experimental conditions directly on the maghemite suspension and pure water. The structure functions and the radial distribution functions for USPIO suspension and water, in the form $\text{Diff}(r)$, are reported respectively in Figure 3 and Figure 4.

Because the iron content was very low (0.30 mol/L), the nanoparticles may be considered as isolated in water. The presence of the organic layer (0.01 mol/L) and the hydration water was negligible due to their small electronic weight with respect to the Fe and the bulk water. In agreement with the definition of the suspension, the experimental structure function of the sample was the sum of two independent contributions:

(23) Božin, E. S.; Petkov, V.; Barnes, P. W.; Woodward, P. M.; Vogt, T.; Mahanti, S. D.; Billinge, S. J. L. *J. Phys.: Condens. Matter*. **2004**, *16*, S5091.
(24) Shin, H. S. *J. Korean Ceram. Soc.* **1998**, *35*, 1113.
(25) Greaves, C. *J. Solid State Chem.* **1983**, *49*, 325.
(26) Murty, B. S.; Datta, M. K.; Pabi, S. K. *Sadhana*. **2003**, *28*, 23.

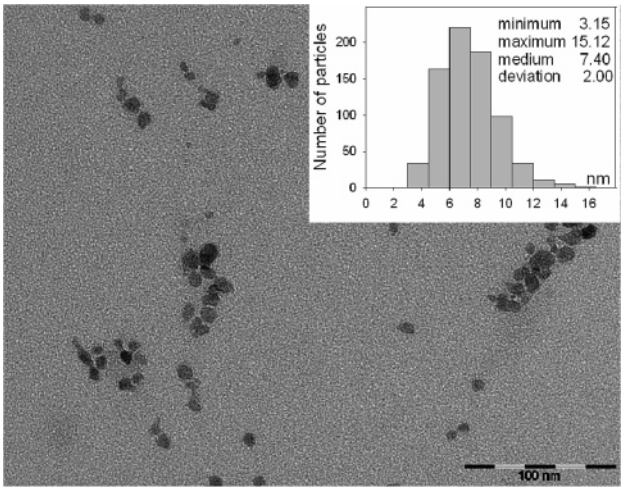

Figure 1. Transmission electron micrograph of USPIO particles. Inset shows the size distribution obtained from the TEM micrograph. Histogram prepared by measuring ca. 750 nanoparticles.

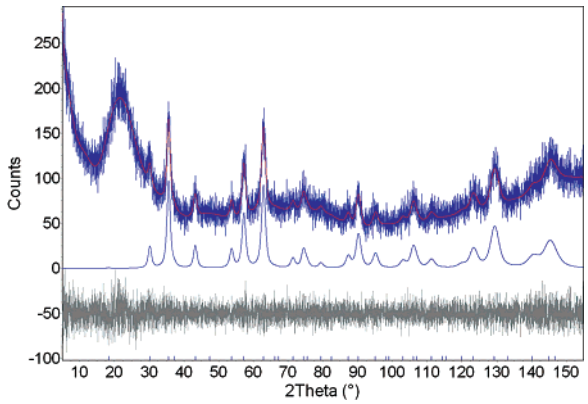

Figure 2. FPA Rietveld refinement of the dried sample. From above to below: experimental (blue), calculated (red), background-subtracted calculated (blue), difference (black) plots. Vertical bars refer to the position of the Bragg reflections.

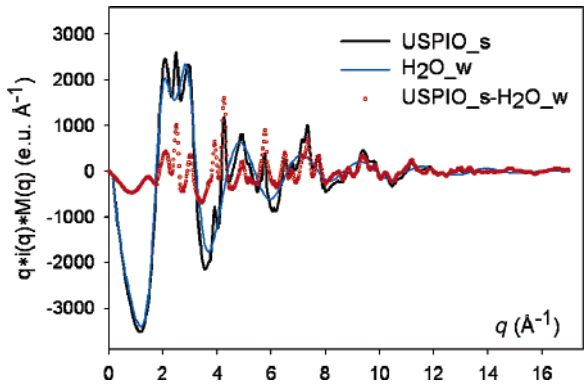

Figure 3. Experimental structure functions in the form $qi(q)M(q)$ of the USPIO suspension (black line, USPIO_s), the weighted water in the suspension (blue line, H_2O_w), and the difference between the suspension and the water (red dots, USPIO_s-H_2O_w).

the water structure function and the maghemite structure function. To characterize the structure of the nanoparticles, the water experimental function, opportunely weighed according to the density difference between pure water and suspension, was subtracted from the experimental one of the USPIO suspension.

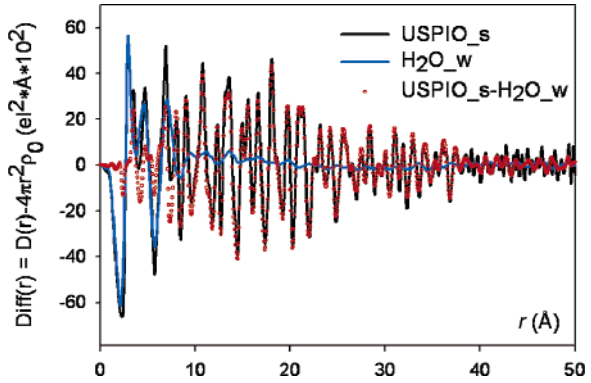

Figure 4. Experimental radial distribution function in the form $\mathrm{Diff}(r) = D(r) - 4\pi r^2\rho_0$ of the USPIO suspension (black line, USPIO_s), the weighted water in the suspension (blue line, H_2O_w), and the difference between the suspension and the water (red dots, USPIO_s-H_2O_w).

The resulting difference functions represented the experimental structure function and the radial distribution function of the iron oxide particles only (Figures 3 and 4). Thus, these functions could be directly compared to the theoretical structure functions obtained from models of iron oxide.

Standard programs calculating the theoretical structure function for systems with a few hundred structured atoms were modified to build up to 25 000 atoms. The models were built on the basis of the structural parameters obtained from ADXD of the dried sample, repeating the unit cell in three dimensions until the required dimensions were obtained. Nanoparticles were modeled in spherical shape as suggested by TEM and ADXD data. The models were built up also taking into account the presence of vacancies at the octahedral sites, distributing them in a partially ordered or random way. To simulate the presence of the randomly distributed vacancies (5/6 site occupancy), the theoretical function was calculated considering the Ti scattering factor ($22e^-$) for all the octahedral cation positions instead of Fe ($26e^-$). The partially structured vacancies were simulated considering the F scattering factor ($9e^-$) in well-defined octahedral cation positions according to a $1 \times 1 \times 3$ supercell. The model with a random distribution gave a reasonable fit with the theoretical functions, whereas that characterized by structured vacancies led to the occurrence of extra peaks and the absence of others with respect to the experimental ones. Consequently, it was deduced that these nanoparticles were characterized by a random or by a very little ordered distribution of vacancies.

Although the apparent size of the particles, as determined from both ADXD and TEM, was of the order of ca. 7.5 nm, we obtained the best correlation using a spherical model with a far smaller diameter. In fact, the experimental and theoretical functions indicated a rigid crystalline structural coherence extending up to 4.2 nm only (Figure 5a and Figure 6a).

Even though the experimental radial distribution function clearly showed a breakdown of both intensity and periodicity of the peaks at ca. 4.0 nm, several models were tested by building nanospheres with diameters ranging from 3.0 to 6.0 nm (i.e., from ca. 3000 to 12 000 atoms). As an example, the theoretical structure function and the radial distribution function, calculated for a sphere with a diameter of 5.0 nm, are reported against the experimental ones (Figures 5b and 6b). As can be seen, the theoretical structure function shows peaks whose

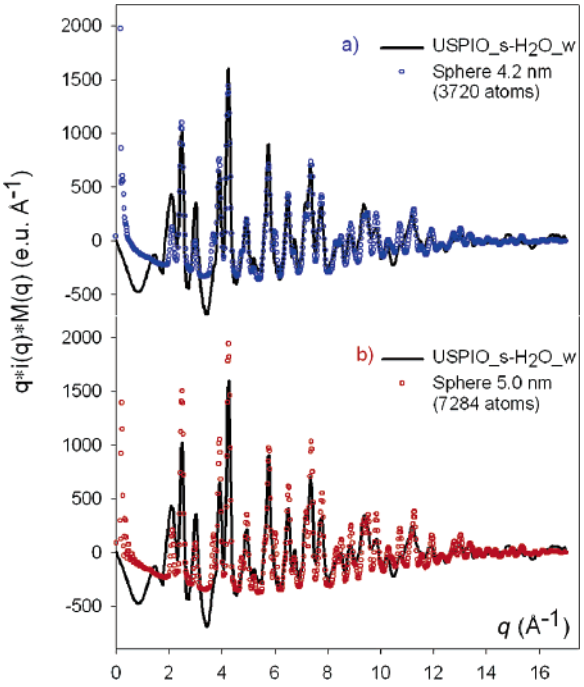

Figure 5. Experimental structure functions in the form $qi(q)M(q)$ of the difference between the suspension and the water (black line) and the theoretical curve calculated for (a) a sphere of 4.2 nm diameter constituted of 3720 atoms (blue dots) and (b) a sphere of 5.0 nm diameter constituted of 7284 atoms (red dots).

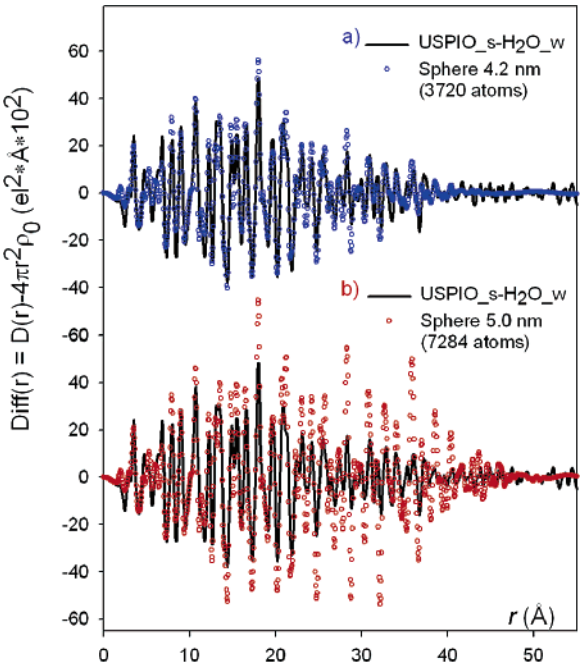

Figure 6. Experimental radial distribution function in the form $\mathrm{Diff}(r) = D(r) - 4\pi r^2\rho_0$ of the difference between the suspension and the water (black line) and the theoretical peak shape function calculated for (a) a sphere of 4.2 nm diameter constituted of 3720 atoms (blue dots) and (b) a sphere of 5.0 nm diameter constituted of 7284 atoms (red dots).

intensities exceed the experimental ones. This effect was even more evident in the theoretical radial distribution function that showed the occurrence of very marked intensity differences starting at 1.8 nm. Supposing that the excessive increase in the height of the peaks could be reduced using larger values for the rms during the calculation of the theoretical function, we tentatively increased the values of the σ well above the values derived from ADXD. As a result, it was possible to achieve a better agreement for some peaks, but at the expense of a significant merging of others resulting in a band structure. Models built up with a more elevated number of atoms required the use of still higher σ values to attenuate the excessive height of peaks that were found also at low r values. Consequently, the peaks located at higher r values became wide bands, occurring as a result of the merging of more peaks.

The presence in the experimental radial distribution function of small peaks at high r values was due to the presence, even though in small quantities, of nanoparticles with a diameter greater than the average (as reported in the TEM particle size distribution), which could possess an extended structural coherence.

Conclusion

Ultrasmall superparamagnetic iron oxide (USPIO) particles play a tremendous role in pharmaceutical contrast agent applications, and as a result, they have often been studied for their magnetic properties, but rarely at the structural particle level. By using a combination of ADXD and EDXD, we succeeded in determining the structural features of the iron oxide nanoparticles. Although both TEM and ADXD show an average crystallite size of ca. 7.5 nm, EDXD indicates a far shorter structural coherence, estimated at ca. 4.0 nm. This means that, from whichever atom, the coherence is restricted to ca. 4.0 nm only, similarly to what happens in liquids and other short-range ordered materials. Within this range, the nanoparticles are characterized by a perfect crystalline coherence, as indicated by the small σ values used, and by a nearly random vacancy distribution, in substantial agreement with reference data.[7] There is no abrupt breakdown in atomic order, but it is present in a three-dimensional lattice distortion due to the effects of defects and finite size. The lattice distortion consists of displacements of the sites away from those of an ordered periodic lattice. The atoms of the particle show a columnar periodicity, but in the three-dimensional lattice, the lattice periodicity is lost faster when, from whichever atom, selected as the origin of the three-dimensional system, the distance increases radially. These kinds of nanocompounds can be defined as disordered crystalline systems or crystals with liquid-like coherence, which is not extended to the whole volume but equal in each volume point without anisotropy. The existence of a structural coherence smaller than the entire volume of the particles, in addition to the disordered surface layer, could be related to their magnetic properties. Therefore, it would be interesting to characterize the structure of similar size nanoparticles with a different saturation magnetization. Our results also suggested that EDXD and ADXD are complementary techniques for the structural characterization of the nanoparticles. In fact, in the case of ADXD, the description of such particles may be carried out in terms of a disordered crystal, whereas in the case of EDXD it is described as a short-range ordered material. Besides this, we have reported here a new application for energy dispersive X-ray diffraction that shows the flexibility of this technique. In fact, we have demonstrated the feasibility of extracting structural data from in situ measurements of suspensions, thus avoiding the risk of modifying the sample.

Acknowledgment. We are grateful to Prof. Ruggero Caminiti, University of Rome "La Sapienza", for his helpful contribution in the modification of the calculation programs and for his stimulating comments and discussions. We also would like to thank Dr. Patricia Beaunier, (SME) University of Pierre et Marie Curie, Paris, for TEM studies. Furthermore, we thank Dr. Caroline Robic and Dr. Isabelle Raynal, and Dr. Irene Guilbert Guerbet SA, for fruitful discussions.

Supporting Information Available: ADXD details. This material is available free of charge via the Internet at http://pubs.acs.org.

JA061674Y